Electronic Supplementary Information

Sensing of Diclofenac by a Porphyrin-based Artificial Receptor

Daniela Intrieri,[a] Caterina Damiano,[a] Silvia Rizzato,[a] Roberto Paolesse,[b] Mariano Venanzi,[b] Donato Monti,*[b] Marco Savioli[b], Manuela Stefanelli[b] and Emma Gallo.*[a]

[a]*Department of Chemistry, University of Milan, Via C. Golgi 19, 20133 Milan (Italy). E-mail: emma.gallo@unimi.it.*

[b]*Department of Chemical Science and Technologies, University of Roma Tor Vergata, Via della Ricerca Scientifica, 00133 Rome (Italy). E-mail: dmonti@uniroma2.it*

1. General

Unless otherwise specified, all the reactions were carried out under a nitrogen atmosphere by employing standard Schlenk techniques and magnetic stirring. Dichloromethane, chloroform, *N,N*-dimethylformamide and pyrrole were distilled over CaH_2 and stored under nitrogen. Acetone was distilled over K_2CO_3 and stored under nitrogen. All the other starting materials and Zn(TPP) were commercial products which were used as received. 2-(3-Bromopropoxy)benzaldehyde[1] and sodium phenylacetate[2] were synthesized by methods reported in the literature or by using minor modifications of them. Solvents used for spectroscopy investigations were of Spectroscopic Grade of the highest degree of purity available and used as received. NMR spectra were recorded at room temperature on a Bruker Avance 400-DRX spectrometers, operating at 400 MHz for ^{1}H, at 100 MHz for ^{13}C and at 376 MHz for [19]F. Chemical shifts (ppm) are reported relative to TMS. The ^{1}H NMR signals of the compounds described in the following have been attributed by COSY and NOESY techniques. Assignments of the resonance in ^{13}C NMR were made using the APT pulse sequence and HSQC and HMBC techniques. UV/Vis spectra were recorded on an Agilent 8453E instrument. Elemental analyses and mass spectra were recorded in the analytical laboratories of Milan University. All spectroscopic studies were carried out at 298.0 ($\pm$ 0.5) K (Julabo F25 Thermostat). Steady-state Fluorescence and Resonance Light Scattering Spectroscopy studies were carried out on Fluoromax 4 (Horiba Instruments). Time-resolved Fluorescence Spectroscopy studies were carried out on LifeSpoec–ps (Edimburg Instruments), equipped with a Hamamatsu Photonics K.K. laser. X-ray data collection was performed at 150 K using graphite-monochromated Mo Kα radiation (λ = 0.71073 Å) on a Bruker ApexII CCD area-detector diffractometer equipped with an Oxford Cryosystems N_2 gas blower. A ω-scan was performed within the Bragg limits of 1.3 < θ < 25.0°. Determination of the integrated intensities and unit cell refinements were performed using SAINT[3] and all absorption corrections were applied by using SADABS.[4] The structures were solved by direct methods (SIR2014)[5] and refined by full-matrix least squares on F^2 (SHELX 2014)[6] with the WINGX interface.[7]

2. Synthetic procedures

2.1. Synthesis of 1.
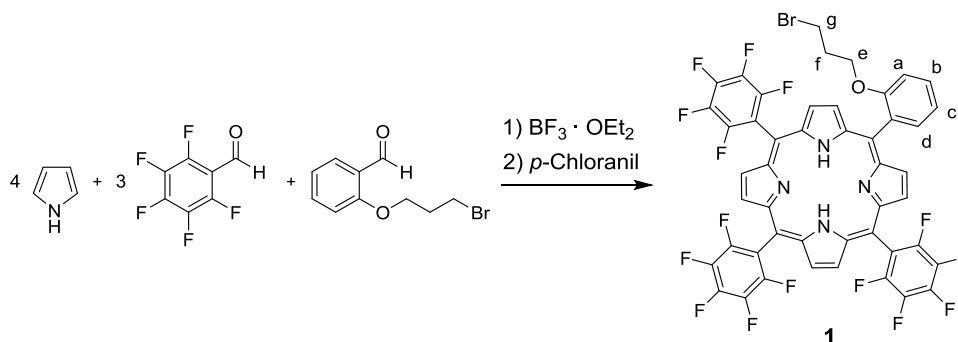
Freshly distilled pyrrole (173 μL, 2.50 mmol), pentafluorobenzaldehyde (231 μL, 1.87 mmol) and 2-(3-bromopropoxy)benzaldehyde (110 μL, 0.62 mmol) were dissolved in dry dichloromethane (250 mL) in a 500 mL two necks round-bottom flask. The reaction mixture was shielded from ambient light and $BF_3 \cdot OEt_2$ (31 μL, 0.25 mmol) was added dropwise by a syringe. The obtained pale orange solution was stirred in the dark for 3 hours at room temperature and then tetrachloro-1,4-benzoquinone (*p*-chloranil) (0.615 g, 2.50 mmol) was added. The resulting solution was refluxed in air for 6 hours, the solvent evaporated to dryness under reduced pressure and the resulting black solid purified by flash column chromatography on silica gel (60 μm, eluent *n*-hexane/dichloromethane = 90:10) yielding **1** (20% yield) as a purple solid. Elemental Analysis calc. for $C_{47}H_{20}BrF_{15}N_4O$: C, 55.26; H, 1.97; N, 5.48; found: C, 55.66; H, 2.11; N, 5.31. UV-Vis, λ_{max} (MeOH)/nm (log ε_M): 410 (5.39), 506 (4.47), 536 (3.61), 582 (3.98), 643 (3.15). LR-MS (ESI): m/z ($C_{47}H_{20}BrF_{15}N_4O$ [M+H]$^+$) calcd. 1020.06; found 1021.2. ^{1}H NMR (400 MHz, $CDCl_3$, 298 K) δ: 8.97 (d, *J* = 4.7 Hz, 2H, H$_{\beta pyrr}$), 8.91 (s, 4H, H$_{\beta pyrr}$), 8.84 (d, *J* = 4.7 Hz, 2H, H$_{\beta pyrr}$), 8.08 (dd, J_o = 7.4 Hz, J_m = 1.5 Hz, 1H, H$_d$), 7.83 (t, *J* = 8.1 Hz, 1H, H$_b$), 7.44 (t, *J* = 7.6 Hz, 1H, H$_c$), 7.38 (d, *J* = 8.1 Hz, 1H, H$_a$), 4.10 (t, *J* = 5.4 Hz, 2H, H$_e$),

2.26 (t, J = 6.0 Hz, 2H, H_g), 1.46 (m, 2H, H_f), -2.81 (s, 2H, NH_{pyrr}). ^{13}C NMR (100 MHz, CDCl$_3$, 298 K) δ: 158.3, 147.8, 145.4, 143.4, 140.9, 138.8, 136.3, 135.6, 130.6, 129.8 (2 signals overlapped), 119.9, 119.4, 116.0, 117.7, 102.8, 101.9, 65.1, 31.3, 29.8. Six quaternary carbon atoms were not detected. ^{19}F NMR (376 MHz, CDCl$_3$, 298 K) δ: -136.9, -152.1, -162.0.

2.2. Synthesis of 2.
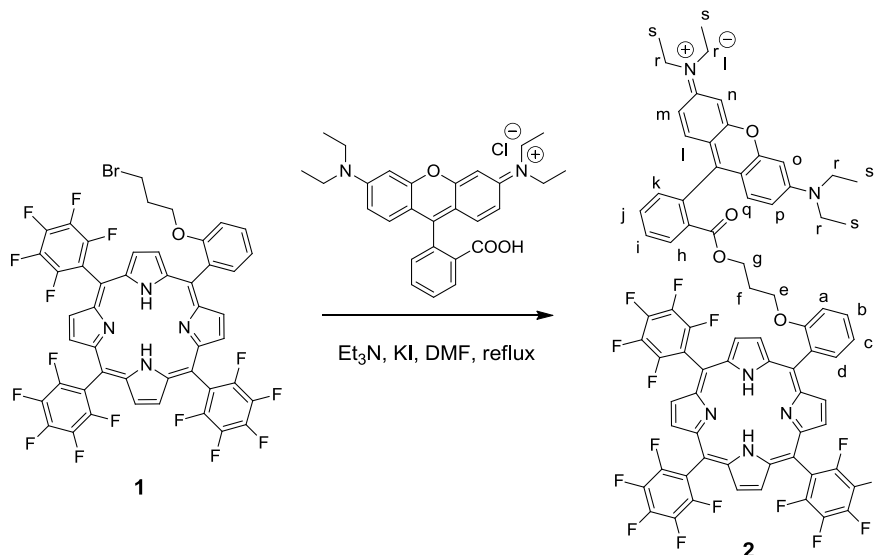
Rhodamine B (0.200 g, 0.418 mmol), triethylamine (58.0 μL, 0.418 mmol) and KI (0.069 g, 0.418 mmol) were added to a dry DMF (25 mL) solution of **1** (0.171 g, 0.167 mmol). The dark purple mixture was refluxed under stirring for 10 hours, then the solvent was evaporated to dryness under reduced pressure and the residue purified by flash column chromatography on silica gel (60 μm, eluent: gradient, from dichloromethane to 3% methanol in dichloromethane) yielding **2** (45% yield) as a dark purple solid (which resulted pink in solution). Elemental Analysis calc. for C$_{75}$H$_{50}$F$_{15}$IN$_6$O$_4$: C, 59.61; H, 3.34; N, 5.56; found: C, 59.93; H, 3.13; N, 5.83. UV-Vis, λ_{max} (MeOH)/nm (log ε_M): 412 (5.67), 512 (4.82), 559 (5.24), 638 (3.18). LR-MS (ESI): m/z (C$_{75}$H$_{50}$F$_{15}$N$_6$O$_4^+$ [M]$^+$) calcd. 1383.36; found 1383.6. ^{1}H NMR (400 MHz, CDCl$_3$, 298 K) δ: 8.87 (m, 6H, H$_{\beta pyrr}$), 8.73 (d, J = 4.3 Hz, 2H, H$_{\beta pyrr}$), 8.00 (dd, J_o = 7.4 Hz, J_m = 1.6 Hz, 1H, H$_d$), 7.78 (m, 2H, H$_b$ and H$_h$), 7.63 (m, 1H, H$_j$), 7.40 (t, J = 7.4 Hz, 2H, H$_c$ and H$_i$), 7.31 (m, 1H, H$_a$), 7.14 (m, 1H, H$_k$), 6.83 (d, J = 9.9 Hz, 2H, H$_l$ and H$_q$), 6.64 (m, 4H, H$_m$, H$_n$, H$_o$ and H$_p$), 3.87 (t, J = 5.5 Hz, 2H, H$_e$), 3.43 (m, 8H, H$_r$), 3.17 (t, J = 6.1 Hz, 2H, H$_g$), 1.13 (m, 14H, H$_f$ and H$_s$), -2.84 (s, 2H, NH_{pyrr}). ^{13}C NMR (100 MHz, CDCl$_3$, 298 K) δ: 164.4, 158.6, 158.1, 157.5, 155.3, 147.8, 145.3, 143.4, 140.9, 138.8, 135.8, 133.2, 132.9, 131.3, 131.1, 131.0, 130.9, 130.1, 129.62, 129.56, 120.0, 119.4, 116.3, 114.2, 113.3, 112.0, 102.7, 96.3, 64.6, 61.9, 46.1, 43.5, 41.3, 36.0, 29.1 27.8, 12.5. ^{19}F NMR (376 MHz, CDCl$_3$, 298 K) δ: -137.0, -140.38, -140.89, -152.0, -161.8.

2.3. Synthesis of 3.
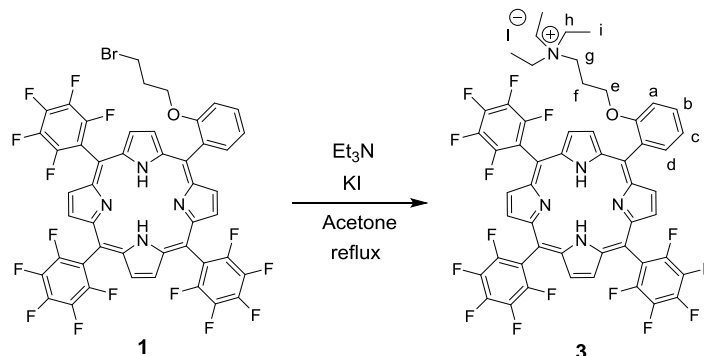
Triethylamine (0.172 mL, 1.24 mmol) and KI (0.207 g, 1.24 mmol) were added to a dry acetone (15 mL) solution of **1** (0.127 g, 0.124 mmol). The dark brown mixture was refluxed under stirring for 6 hours, then

the solvent evaporated to dryness under reduced pressure and the resulting solid purified by flash column chromatography on silica gel (60 μm, eluent: gradient, from dichloromethane to 3% methanol in dichloromethane) yielding **3** (55% yield) as a dark red solid. Elemental Analysis calc. for $C_{53}H_{35}F_{15}IN_5O$: C, 54.42; H, 3.02; N, 5.99; found: C, 54.23; H, 3.11; N, 6.06. UV-Vis, λ_{max} (CH_2Cl_2)/nm (log ε_M): 413 (5.49), 507 (4.28), 536 (3.47), 583 (3.80), 636 (3.14). λ_{max} (MeOH)/nm (log ε_M): 409 (5.49), 505 (4.27), 535 (3.39), 580 (3.76), 635 (2.96). LR-MS (ESI): m/z ($C_{53}H_{35}F_{15}N_5O^+$ [M]$^+$) calcd. 1042.26; found 1042.4. ^{1}H NMR (400 MHz, CDCl$_3$, 298 K) δ: 8.96 (m, , 6H, H$_{\beta pyrr}$), 8.89 (d, J = 4.5 Hz, 2H, H$_{\beta pyrr}$), 8.22 (dd, J_o = 7.6 Hz, J_m = 1.5 Hz, 1H, H$_d$), 7.86 (t, J = 8.0 Hz, 1H, H$_b$), 7.54 (t, J = 7.6 Hz, 1H, H$_c$), 7.34 (d, J = 8.0 Hz, 1H, H$_a$), 3.96 (t, J = 4.8 Hz, 2H, H$_e$), 1.29 (m, 2H, H$_f$), 0.97 (q, J = 6.9 Hz, 6H, H$_h$), 0.6 (m, 2H, H$_g$), -1.26 (t, J = 6.9 Hz, 9H, H$_i$), -2.94 (s, 2H, NH_{pyrr}). ^{13}C NMR (100 MHz, CDCl$_3$, 298 K) δ: 162.8, 158.5, 148.5, 145.4, 140.0, 136.4, 134.2, 131.7, 130.8, 121.5, 119.8, 114.5, 103.3, 65.8, 52.7, 51.5, 22.4, 5.2. Eight quaternary carbon atoms were not detected. ^{19}F NMR (376 MHz, CDCl$_3$, 298 K) δ: -137.8, -151.0, -161.0.

2.4. Synthesis of Zn(2).
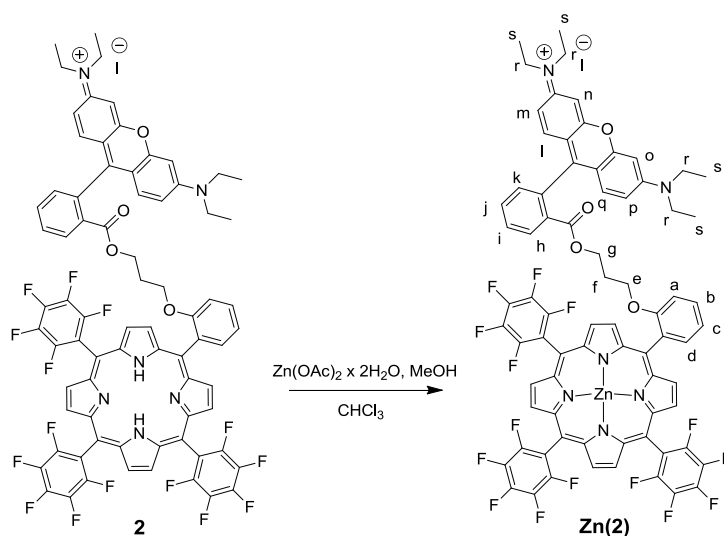
A dry CH$_3$OH (13.50 mL) solution of Zn(OAc)$_2$·2H$_2$O (72 mg, 0.33 mmol) was added to a CHCl$_3$ (6.50 mL) solution of **2** (49 mg, 0.033 mmol) in a 50 mL dried Schlenk. The mixture was refluxed under stirring for 2 hours, then the solvent was evaporated to dryness under reduced pressure and 15 mL of CH$_2$Cl$_2$ was added to the residue. The organic phase was washed with water (3 x 15 mL), dried over NaSO$_4$ and the filtrate was evaporated to dryness under reduced pressure yielding Zn(**2**) in a quantitative yield. Elemental Analysis: calc. for $C_{75}H_{48}F_{15}IN_6O_4Zn$: C, 62.23; H, 3.34; N, 5.81; found: C, 62.40; H, 3.71; N, 5.62. UV-Vis, λ_{max} (CH$_2$Cl$_2$)/nm (log ε_M): 419 (5.05), 560 (4.99). λ_{max} (MeOH)/nm (log ε_M): 418(5.01), 561(4.83). LR-MS (ESI): m/z ($C_{75}H_{48}F_{15}N_6O_4Zn^+$ [M]$^+$) calcd. 1445.28; found 1446.67. ^{1}H NMR (400 MHz, CDCl$_3$, 298 K): δ 8.91 (m, 6H, H$_{\beta pyrr}$), 8.75 (s, 2H, H$_{\beta pyrr}$), 8.14 (d, J = 6.7 Hz, 1H, H$_h$), 7.76 (t, J=7.6 Hz, 1H, H$_j$), 7.44 (br s, 2H, H$_i$ and H$_a$), 7.26 (br s, H$_k$ and H$_c$), 7.13 (br s, 1H, H$_b$), 6.88 (d, J=7.4 Hz, 1H, H$_d$), 6.53 (s, 2H, H$_l$ and H$_q$), 6.41 (m, 4H, H$_m$, H$_n$, H$_o$ and H$_p$), 3.48 (s, 2H, H$_e$), 3.38 (br s, 8H, H$_r$), 1.28 (solvent overlap H$_g$), 1.12 (s, 12H, H$_s$), 0.62 (s, 2H, H$_f$). ^{13}C NMR (100 MHz, CDCl$_3$, 298K): δ 158.8, 157.9, 157.3, 155.3, 151.3, 150.1, 149.8, 149.6, 148.3, 145.0, 135.1, 133.6, 132.7, 132.5, 132.4, 131.6, 131.2, 130.7, 130.4, 129.8, 129.7, 120.8, 114.0, 113.0, 103.1, 102.3, 96.4, 66.1, 61.8, 46.1, 29.8, 27.2, 12.6. eight quaternary carbon atoms were not detected. ^{19}F NMR (376 MHz, CDCl$_3$, 298 K): δ -136.7, -137.7, 140.3, 141.3, 152.4, -153.1, -162.3 to -163.0.

4

3. ^{1}H, ^{13}C and ^{19}F NMR spectra of reported compounds

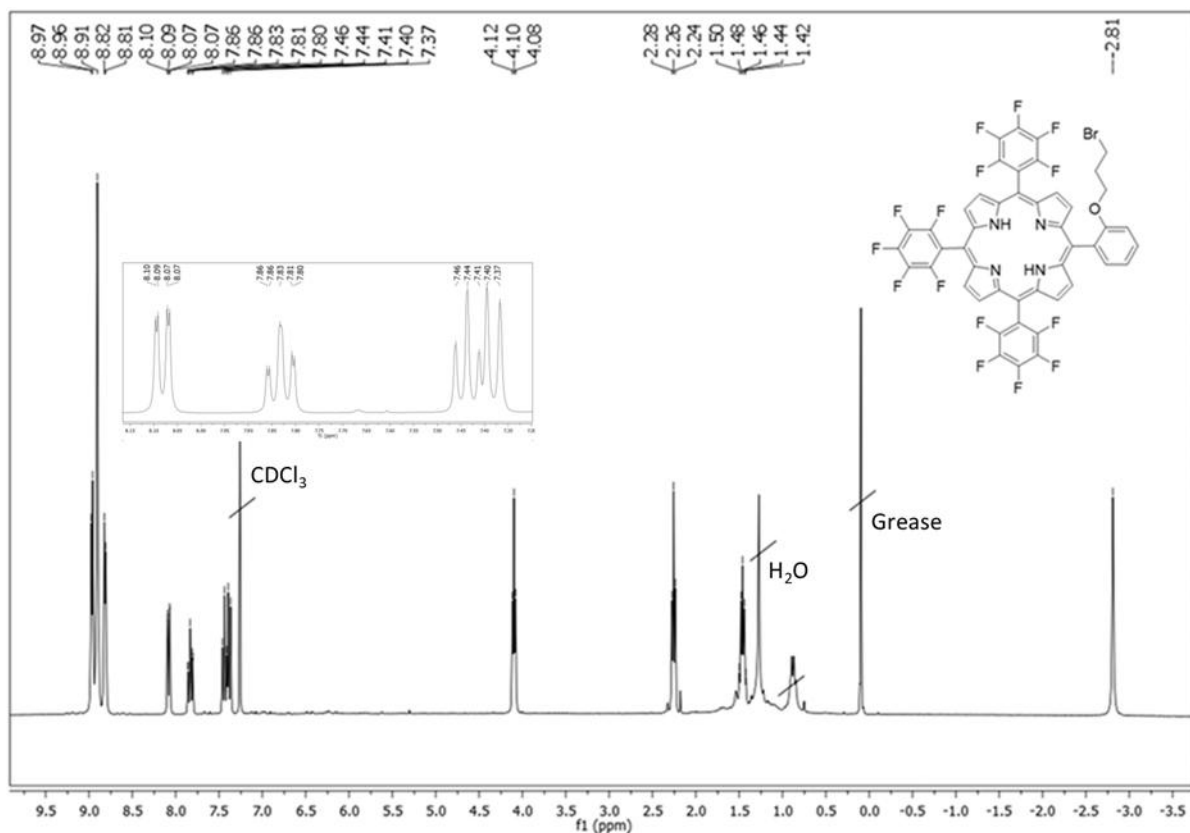Figure 1. ^{1}H NMR spectrum (400 MHz, CDCl$_3$, 298 K) of porphyrin **1**

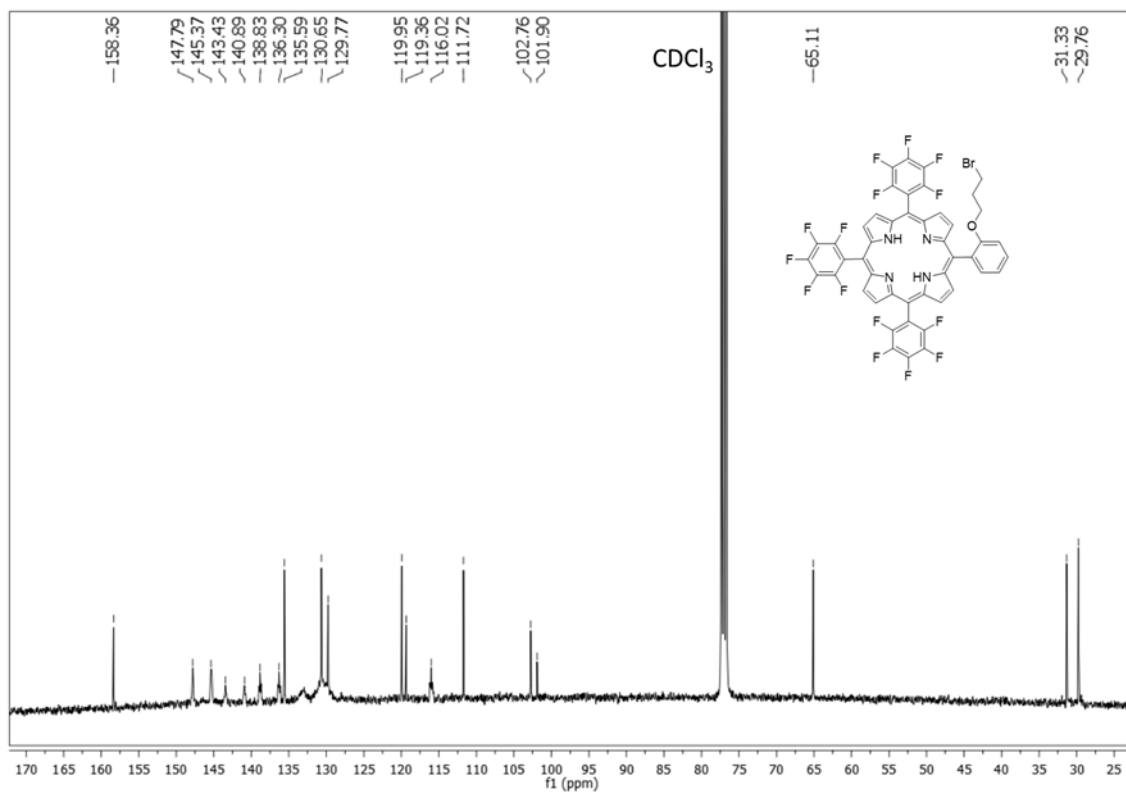Figure 2. ^{13}C NMR spectrum (100 MHz, CDCl$_3$, 298 K) of porphyrin **1**

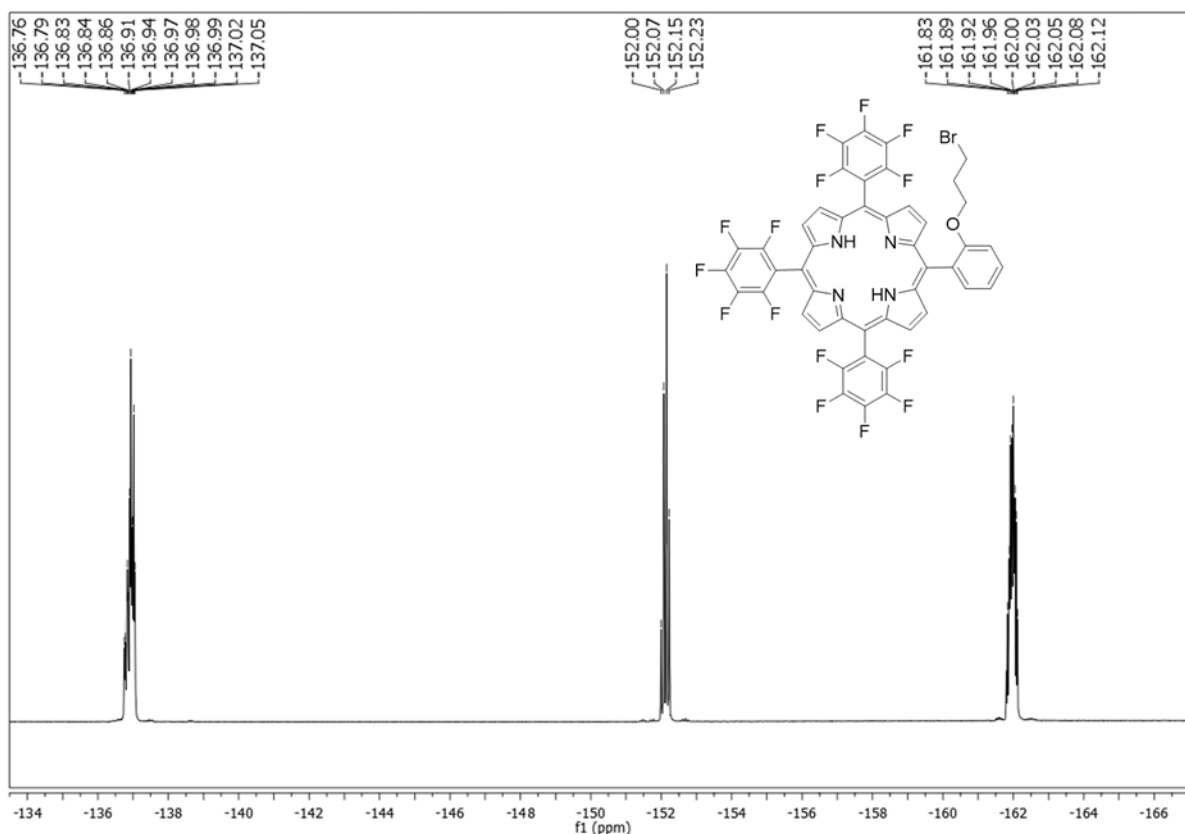Figure 3. ^{19}F NMR spectrum (376 MHz, CDCl$_3$, 298 K) of porphyrin **1**

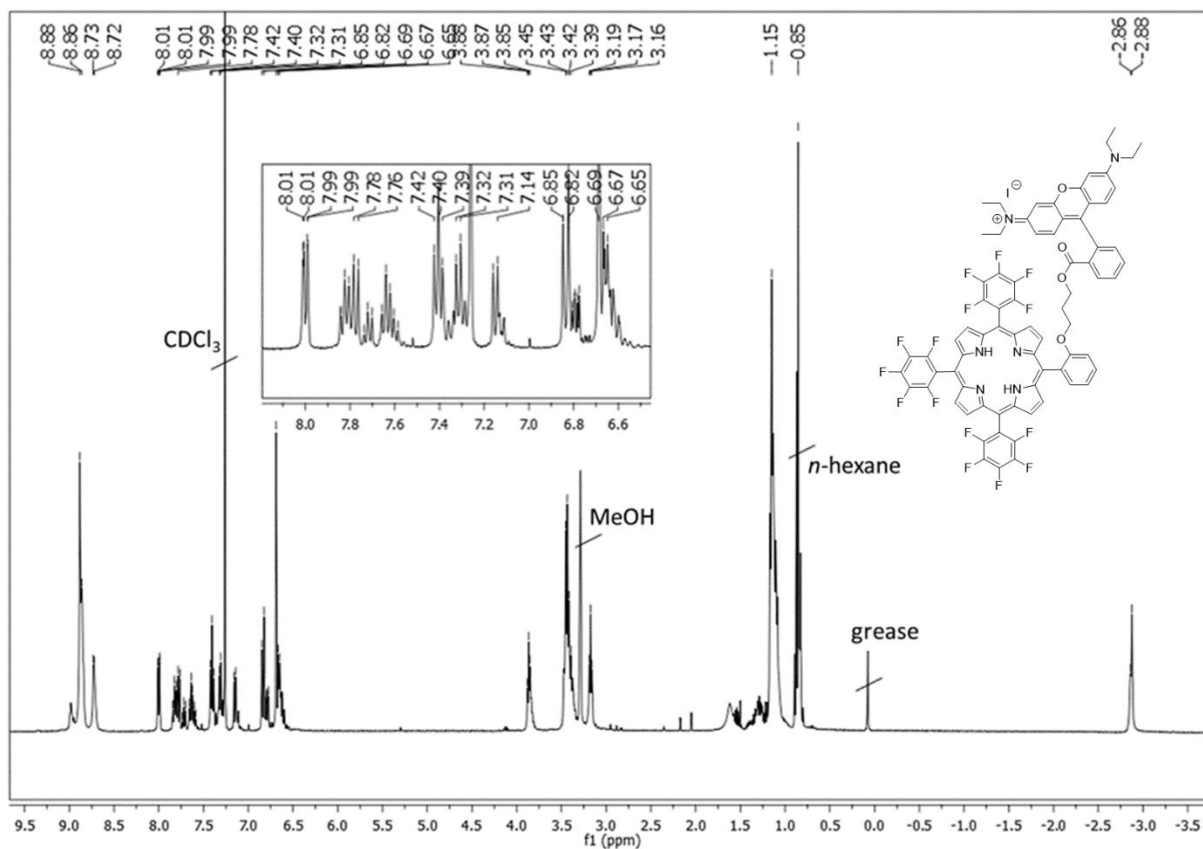Figure 4. ^{1}H NMR spectrum (400 MHz, CDCl$_3$, 298 K) of porphyrin **2**

Figure 5. ^{13}C NMR spectrum (100 MHz, CDCl$_3$, 298 K) of porphyrin **2**
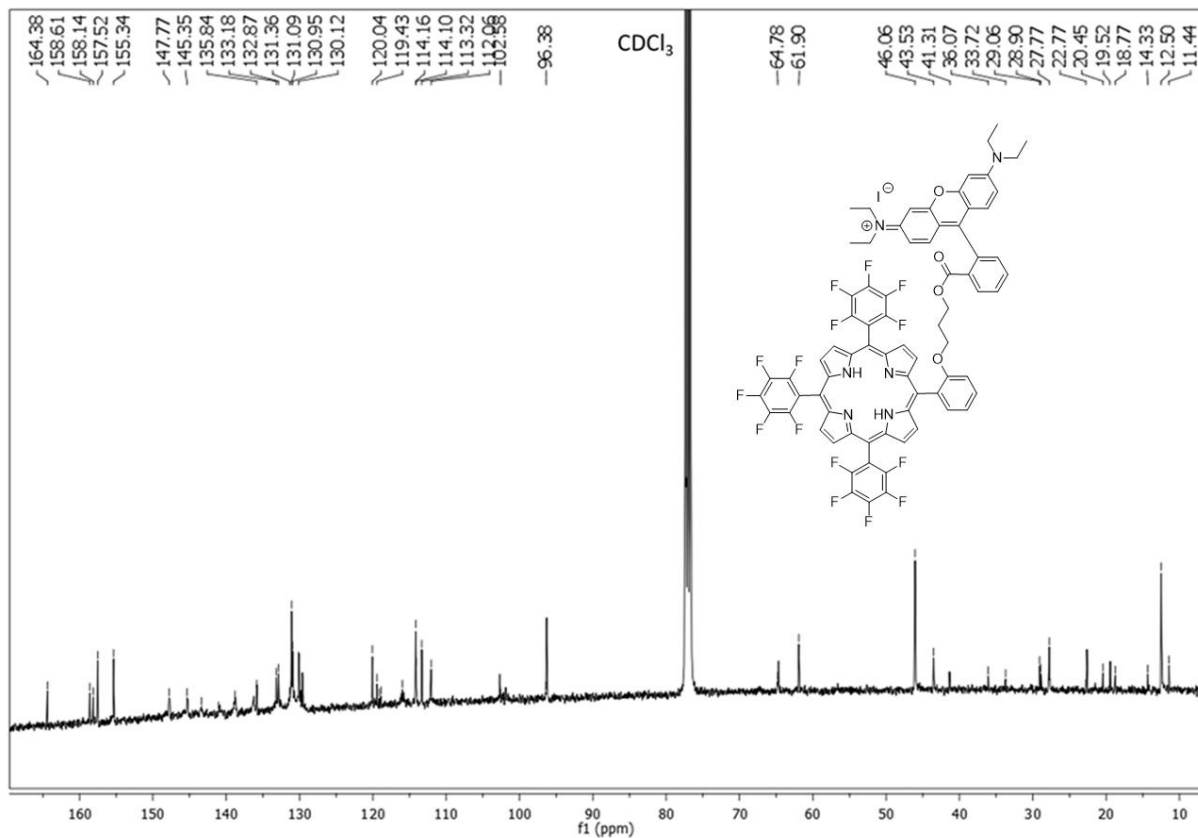

Figure 6. ^{19}F NMR spectrum (376 MHz, CDCl$_3$, 298 K) of porphyrin **2**
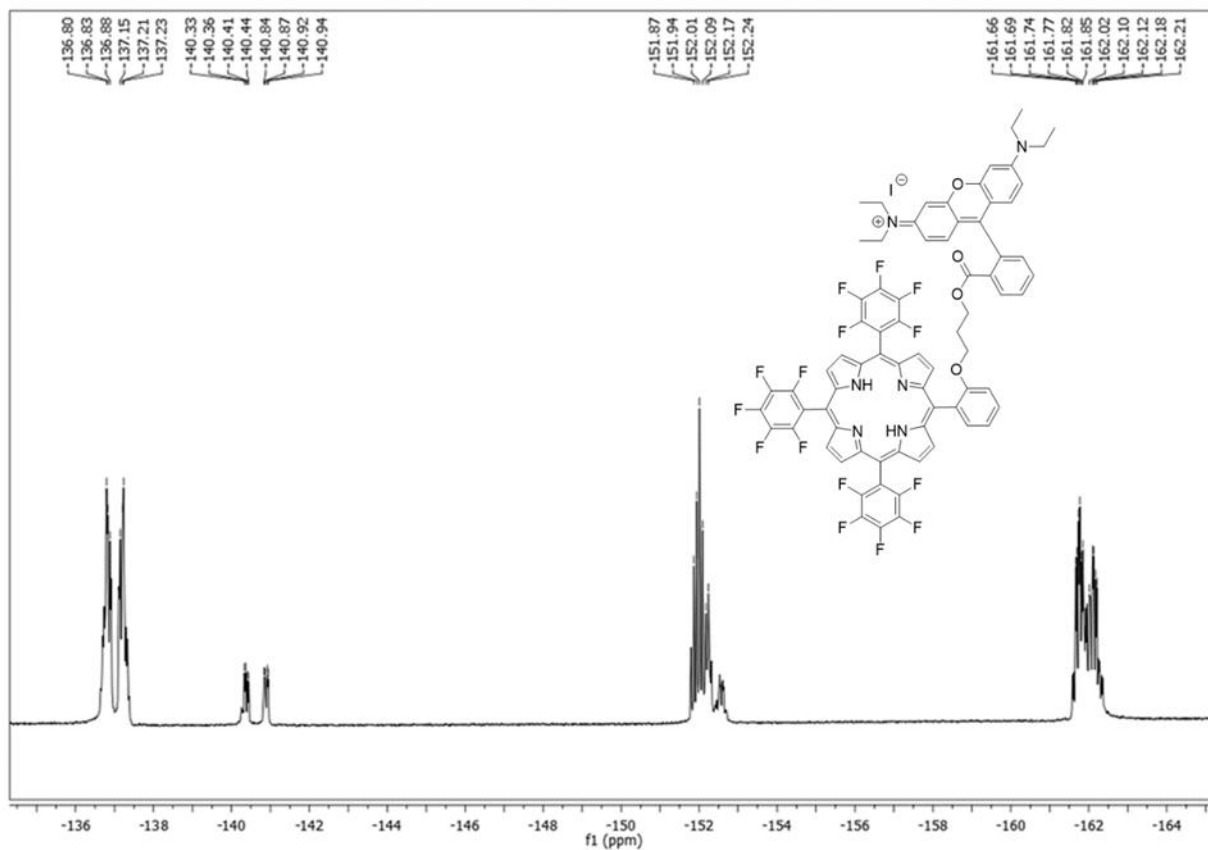
Figure 7. ^{1}H NMR spectrum (400 MHz, CDCl$_3$, 298 K) of porphyrin **3**
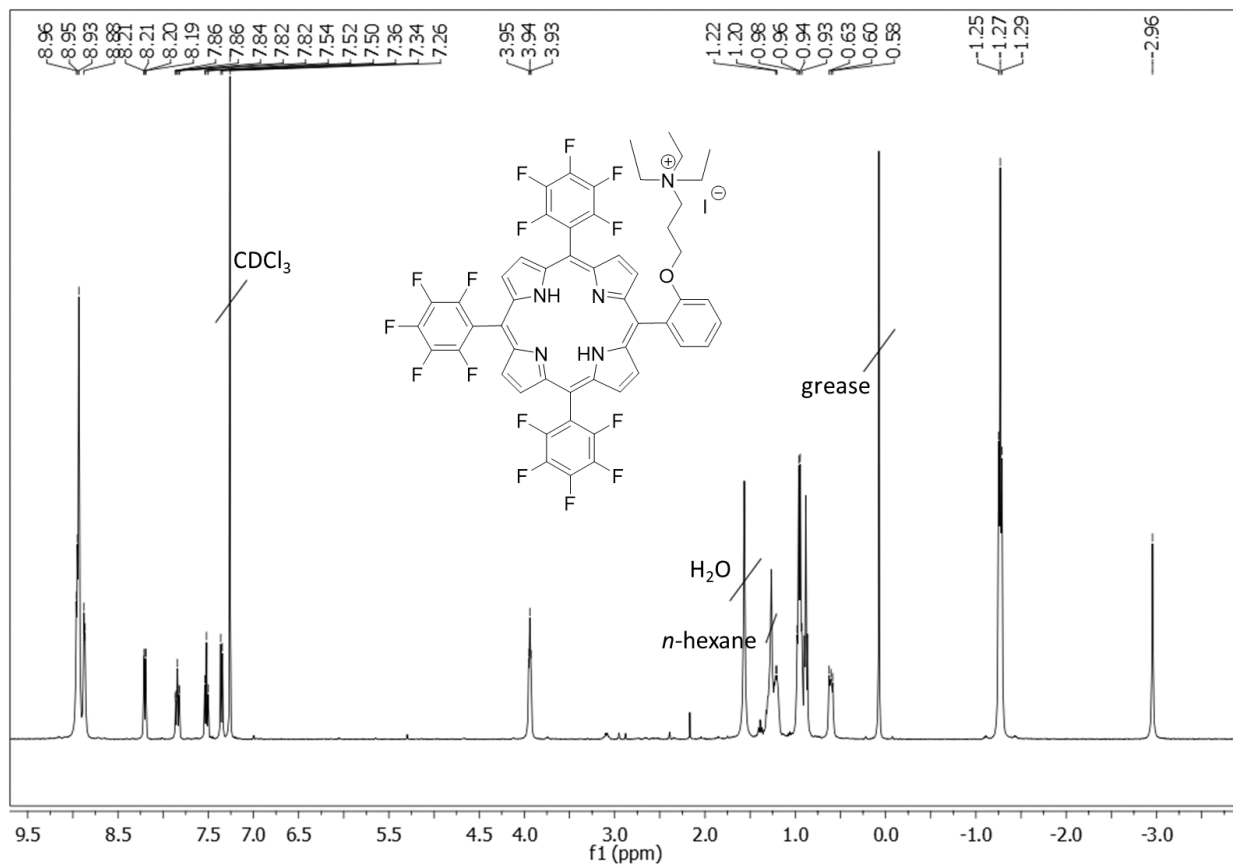

Figure 8. ^{13}C NMR spectrum (100 MHz, CDCl$_3$, 298 K) of porphyrin **3**
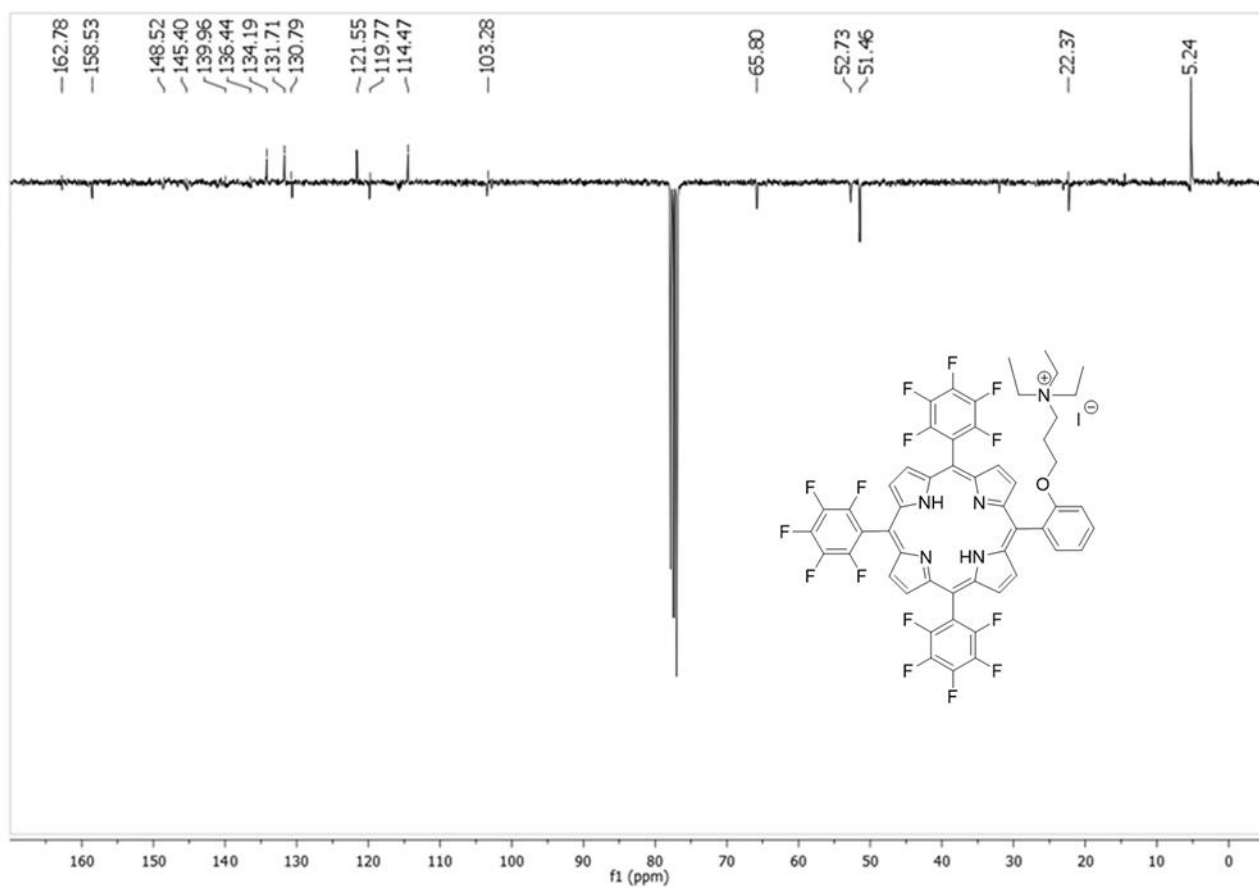
Figure 9. ^{19}F NMR spectrum (376 MHz, CDCl$_3$, 298 K) of porphyrin **3**
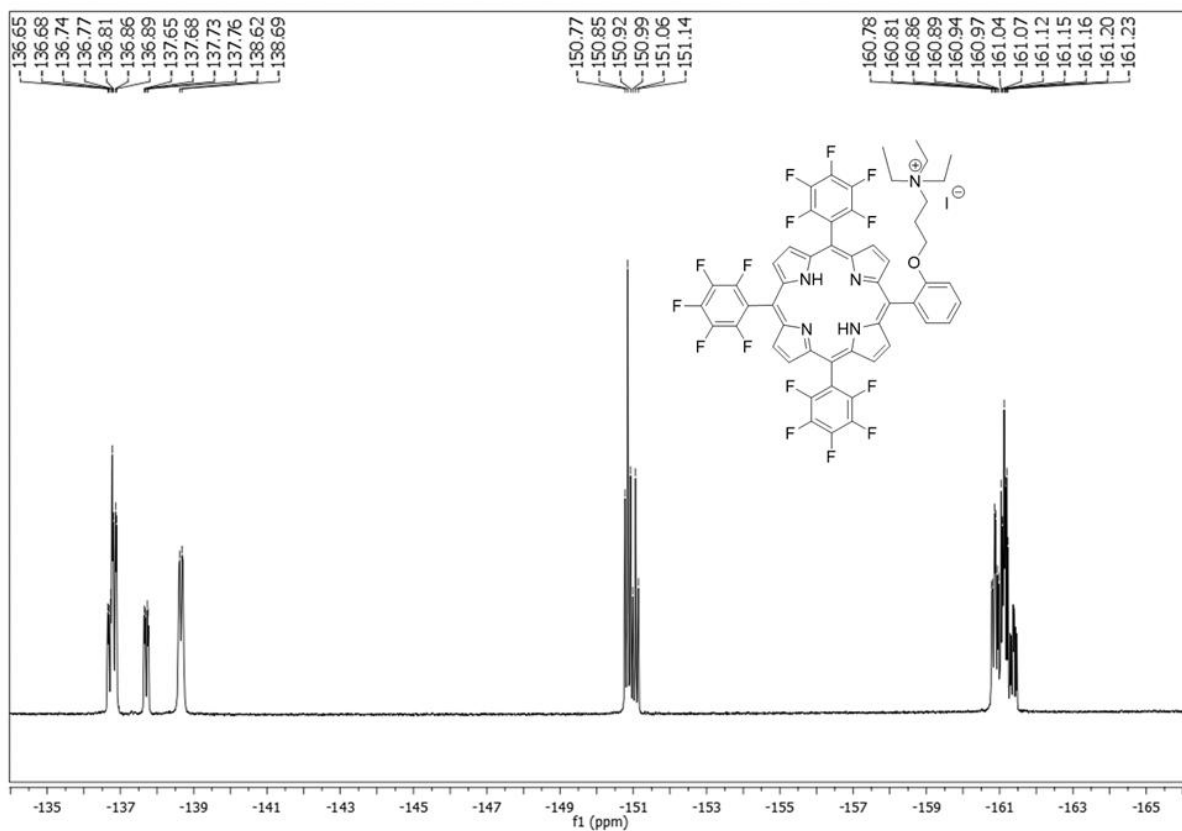

Figure 10. ^{1}H NMR spectrum (400 MHz, CDCl$_3$, 298 K) of porphyrin Zn(**2**)
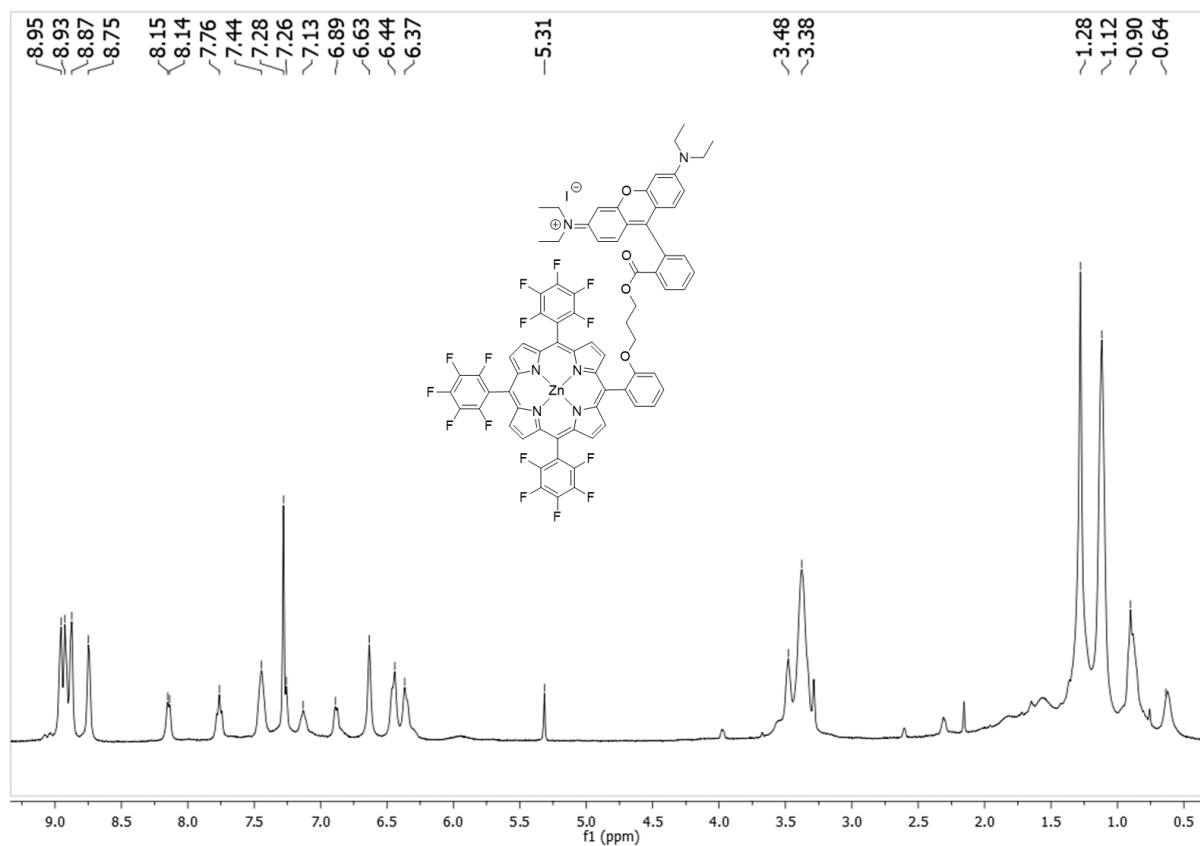
Figure 11. ^{13}C NMR spectrum (100 MHz, CDCl$_3$, 298 K) of porphyrin Zn(**2**)
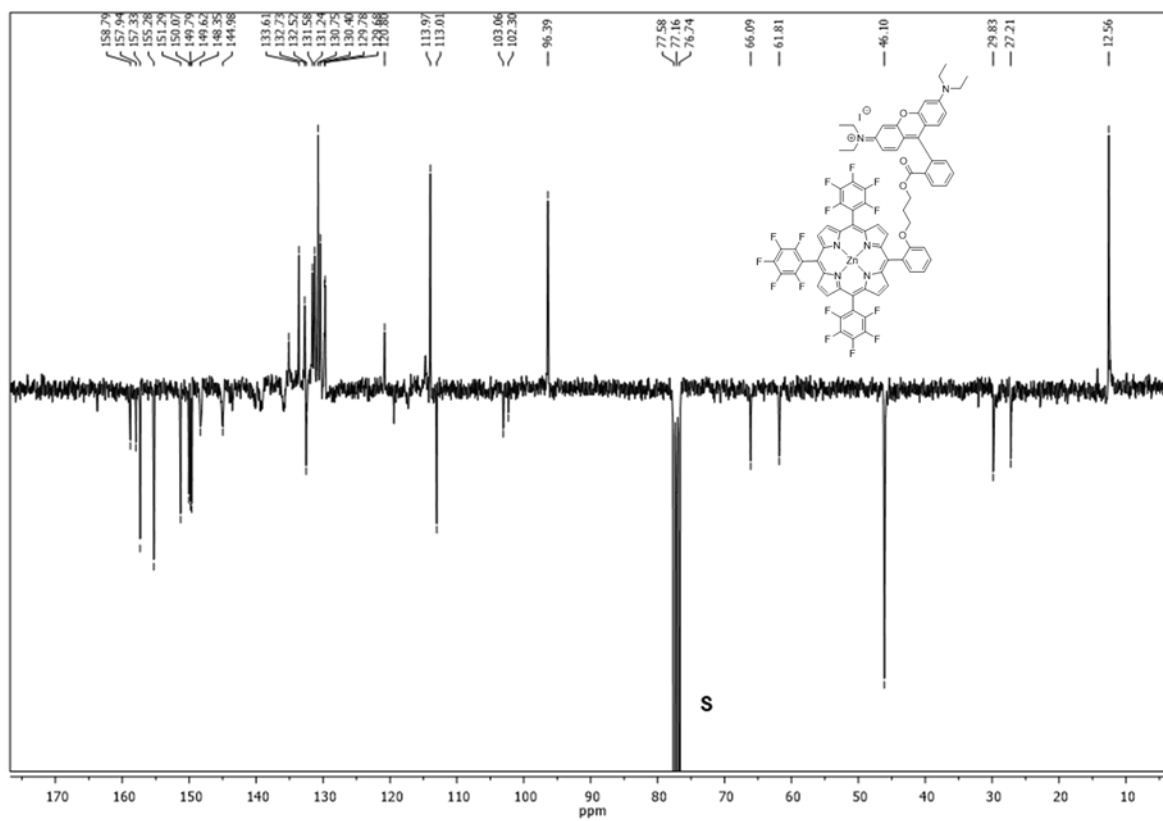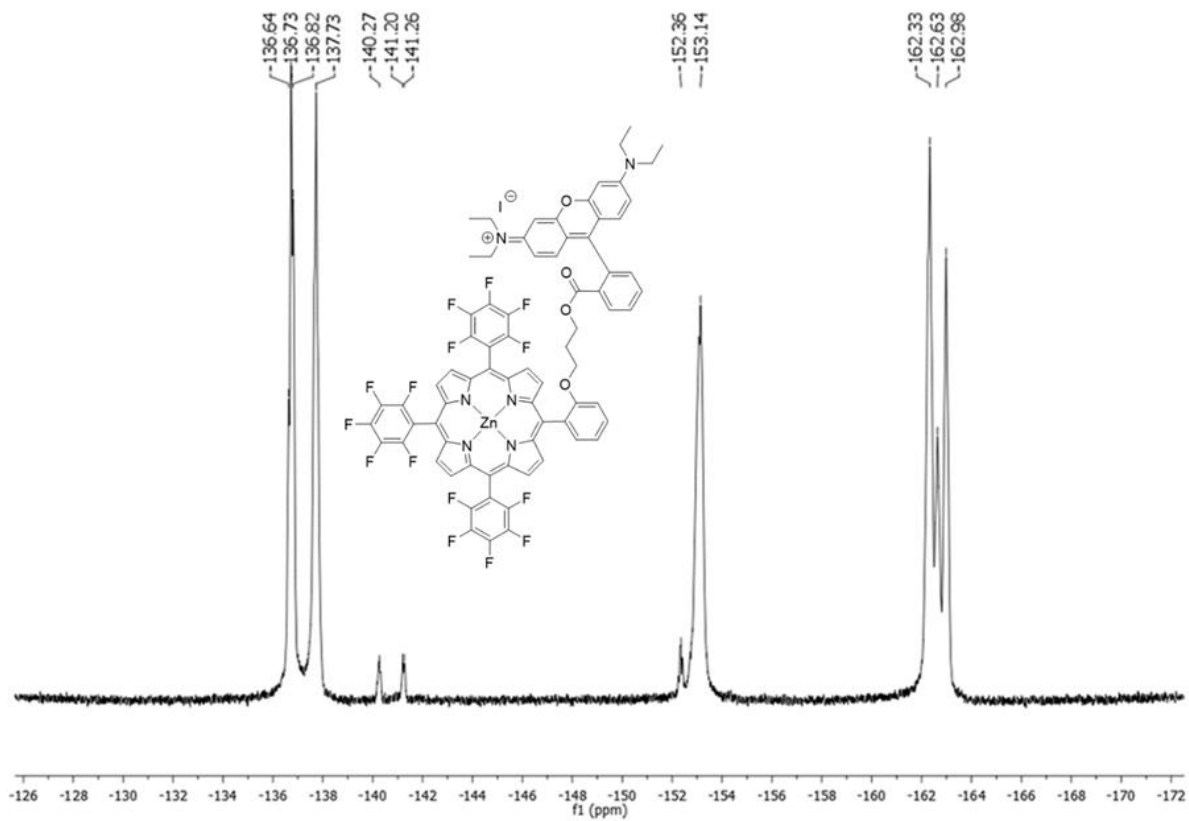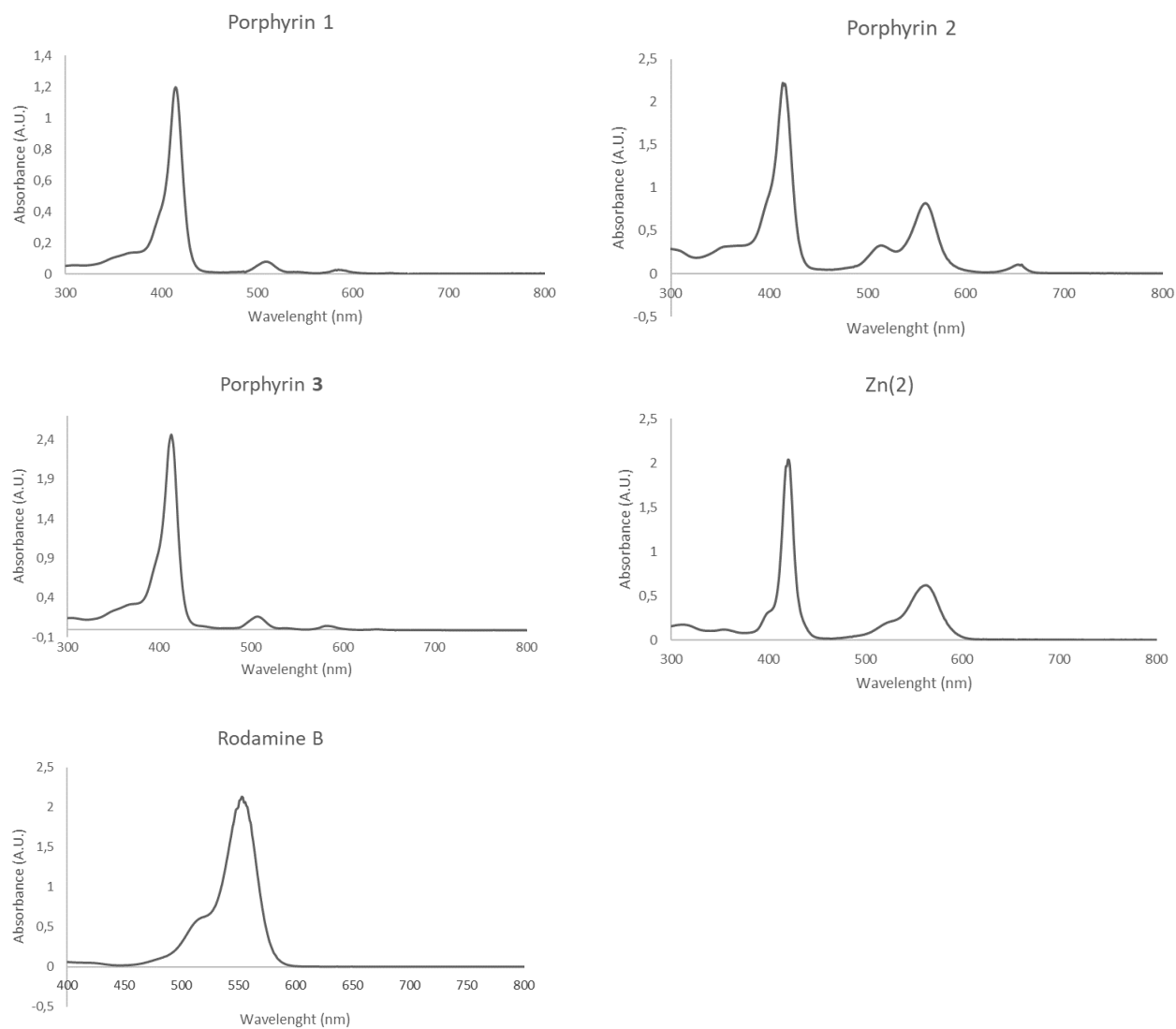

Figure 12. ^{19}F NMR spectrum (376 MHz, CDCl$_3$, 298 K) of porphyrin Zn(**2**)

4. UV-Vis spectra

Figure 13. UV-vis spectra of **1**, **2**, **3**, Zn(**2**) and Rhodamine B in MeOH.

5. UV-Vis binding tests

Binding constant measurements were carried out on a Cary 100 Spectrophotometer at 298.0 (± 0.5) °C by adding consecutive aliquots of a (DCF)Na solution (1.00 mM) to 2.0 mL of 1:1 MeOH/H$_2$O (v:v) receptor (**2** or Zn(**2**)) solution (10.0 μM). The corresponding spectra was acquired after every (DCF)Na addition. The (DCF)Na solution was prepared by dissolving the required amount of salt into 10.0 mL of 10.0 μM porphyrin solution, in order to keep the concentration of the receptor to a constant value throughout the titration. The absorbance values at 419 nm were plotted against (DCF)Na concentration and acquired data fitted to Equation 1[8] for a 1:1 molecular complex formation by using a non-linear regression fit program (KaleidaGraph ® 4.1 Synergy Software). Experiments were performed in duplicate and obtained results showed a very good reproducibility. The same procedure was followed in the presence of sodium phenylacetate, sodium salicylate, L tyrosine sodium salt, sodium sarcosinate, L-alanine sodium salt as well as for Fluorescence and Resonance Light Scattering (RLS) studies.

Equation 1

$$\frac{A_0 - A}{A - A_\infty} = \frac{[S]_t + [L]_a + 1/K_{binding} - \sqrt{\left([S]_t + [L]_a + 1/K_{binding}\right)^2 - 4[S]_t[L]_a}}{2[S]_t}$$

Figure 14. UV-vis binding test with porphyrin **2**
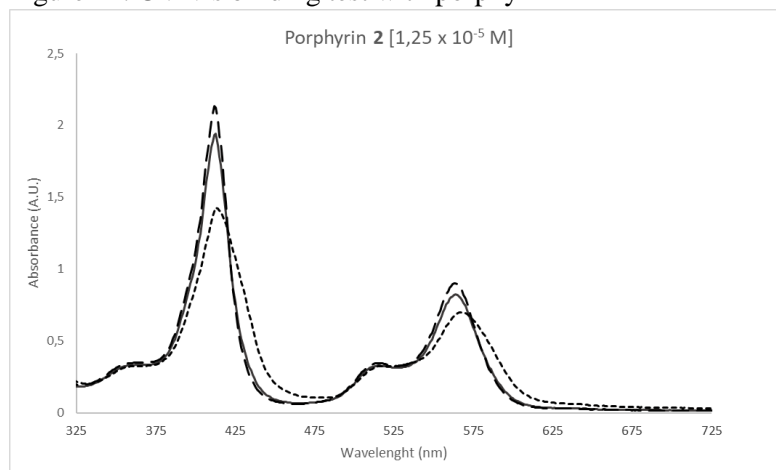
Figure 15. UV-vis binding test with porphyrin Zn(**2**)
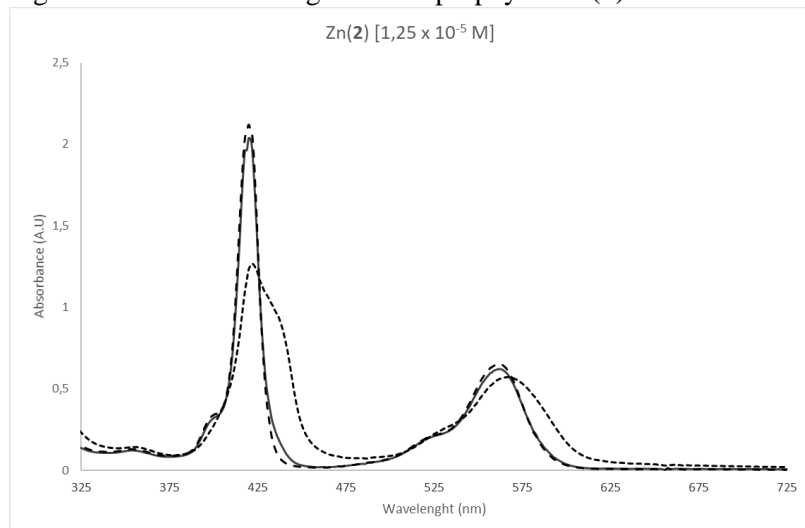
Figure 16. UV-Vis spectral pattern variation of **2** (10 μM; MeOH/H$_2$O 1:1 v:v) upon addition of (DCF)Na and equimolar amount of sodium salicylate (SalONa).
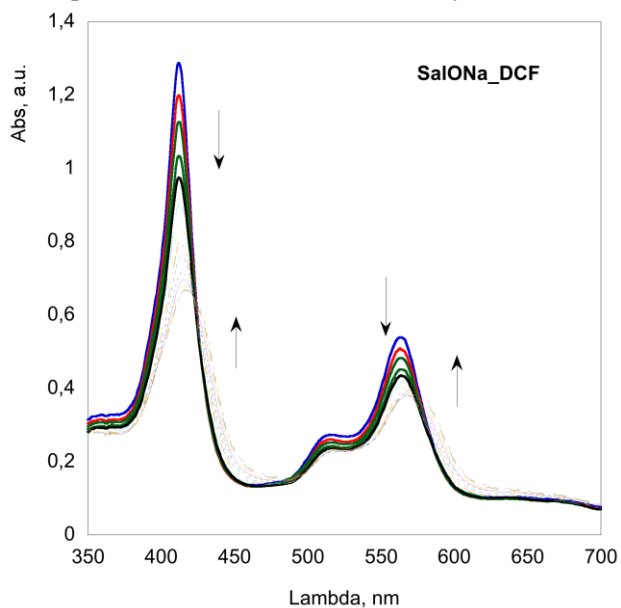
Figure 17. Non-linear regression fit, and calculated binding constant value (Langmuir type equation, see above) for the **2@DCF** formation in the presence of equimolar amount of sodium salicylate.
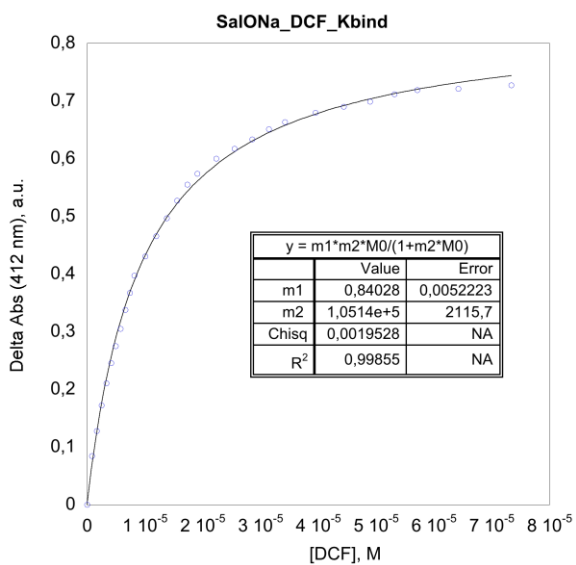
6. Fluorescence experiments

Figure 18. Fluorescence emission spectrum of **2** at λ_{exc} = 412 nm.
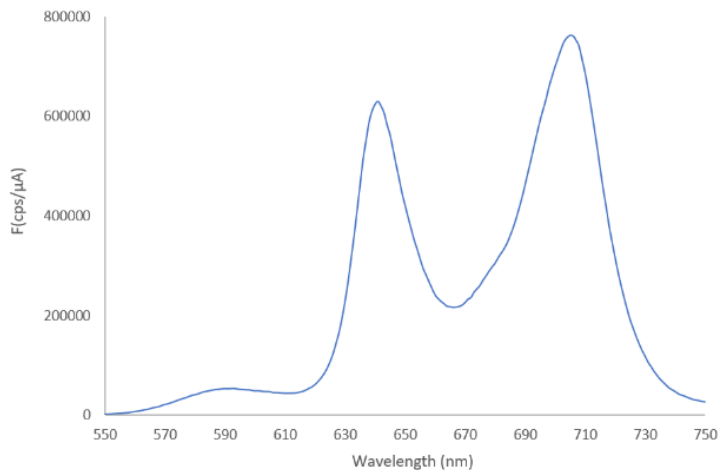
Figure 19. Fluorescence excitation spectrum of **2** at λ_{em}=590 nm (Rhodamine emission)
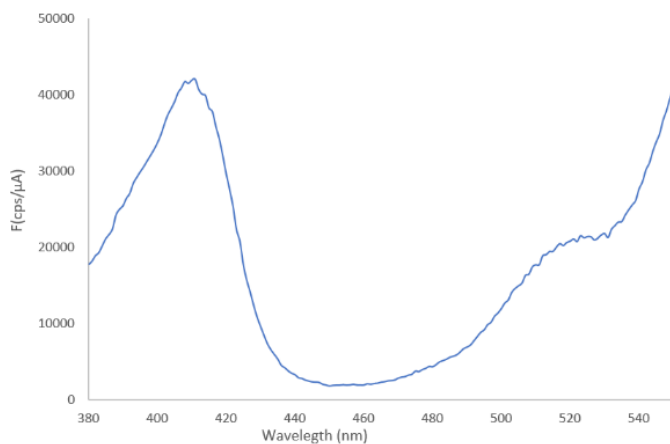
Figure 20. Fluorescence excitation spectrum of **2** at λ_{em}=705 nm (Porphyrin emission)
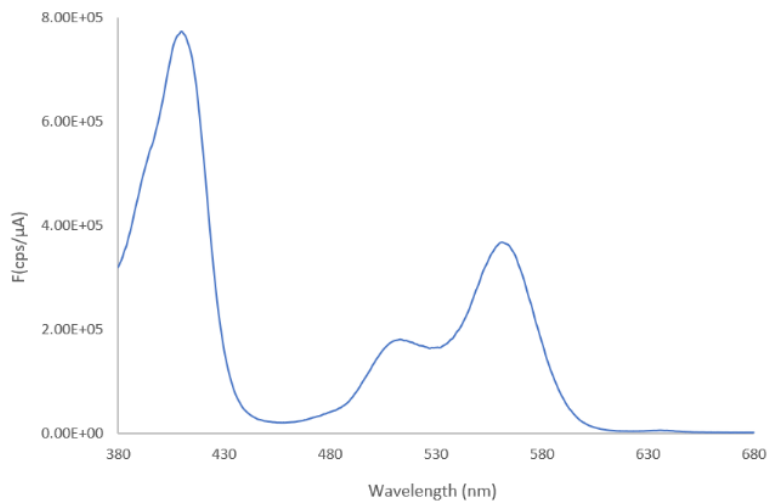
Figure 21. Fluorescence emission spectra of **2** for increasing concentrations of DCF. **A**: λ_{ex}=412 nm (Porphyrin absorption); **B**: λ_{ex}=555 nm (Rhodamine preferential absorption).
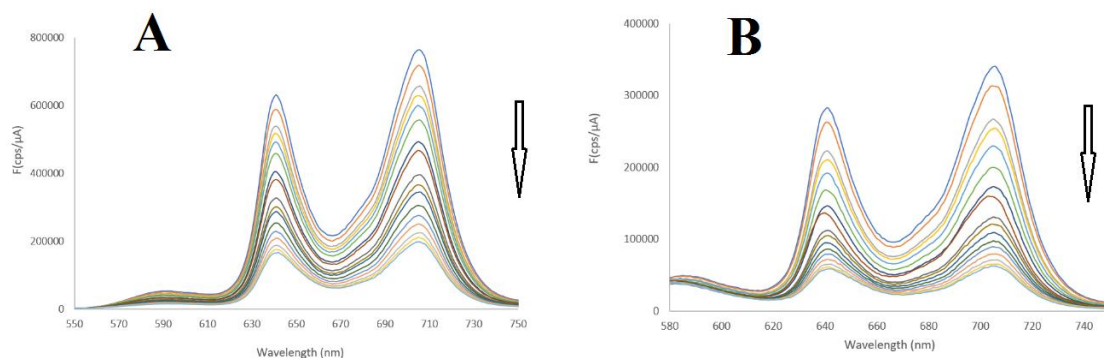
Figure 22. **2**/DCF binding isotherm from fluorescence intensities of **2** for different (DCF)Na concentrations. The analogous of Equation 1 was applied.
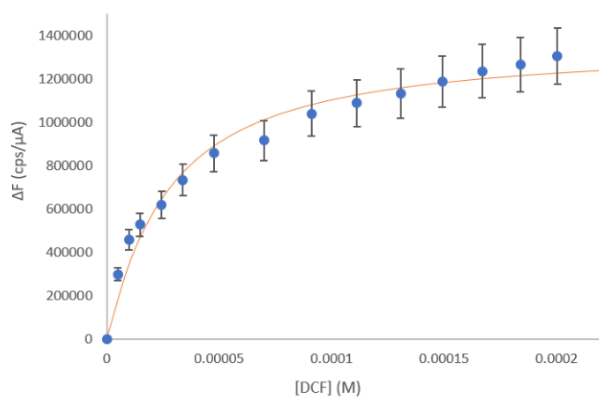
Figure 23. Fluorescence time decays of **2** for different **2**/DCF concentration ratios (λ_{ex}=342 nm; λ_{em}=645 nm).
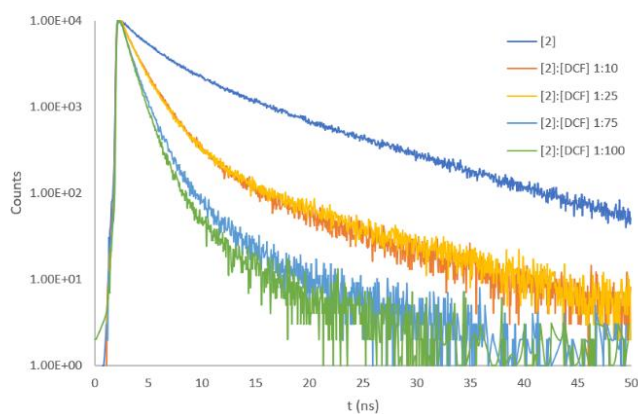
Table 1. Time decay parameters of **2** (porphyrin emission) for different **2**/DCF concentration ratios (λ_{ex}=342 nm; λ_{em}=645 nm).

[2]:[DCF]	τ_1 (ns)	α_1	τ_2 (ns)	α_2	τ_3 (ns)	α_3	$<\tau>$ (ns)	χ^2
1:0	11.6	0.38	3.45	0.46	1.0	0.17	6.3	1.303
1:10	10.2	0.02	2.2	0.52	0.95	0.46	1.8	1.154
1:25	10.0	0.03	2.1	0.48	0.88	0.49	1.7	1.031
1:75	6.1	0.01	1.5	0.41	0.72	0.58	1.1	1.052
1:100	5.0	0.01	1.2	0.50	0.64	0.49	1.0	0.913

7. X-ray single-crystal structure determination.

Crystal data for **3** are reported in Table 2. All hydrogen atoms of porphyrin molecule, except the H atoms of methyl groups, were located from the difference Fourier map and refined freely with isotropic displacement *parameters*. Methyl hydrogens and H-atoms of the guest molecule (*n*-hexane) were placed in geometrically calculated positions and included in the refinement using a riding model in conjunction with a $U_{iso}(H) = 1.2$ $U_{eq}(CH_2, CH)$ or $1.5U_{eq}(CH_3)$ constraint. All non-hydrogen atoms were *refined with* full occupancy and *anisotropic displacement parameters* except for hexane carbon atoms. ISOR instruction was used for F2 atom as otherwise it went non-positive definite. The solvate hexane molecule was find to be disordered and refined isotropically over two positions using a suitable model (49.7, 50.1%). Geometry constraints (SADI) were used to keep reasonable bond distances.

Table 2. Crystal data and structure refinement for **3**.

Chemical formula	$[C_{53}H_{35}F_{15}N_5O]I \cdot 0.5(C_6H_{14})$
Empirical formula	$C_{56} H_{42} F_{15} I N_5 O$
Formula weight (g·mol^{-1})	1212.85
Temperature (K)	150(2)
Wavelength (Å)	0.71073
Crystal system	Triclinic
Space group	*P* -1
a / Å	11.465(3)
b / Å	15.353(4)
c / Å	16.170(5)
α (deg)	103.382(3)
β (deg)	90.662(3)
γ (deg)	106.684(3)
V / Å^3	14687(2)
Z	12
$D_{calc.}$ (g·cm^{-3})	1.524
μ (mm^{-1})	0.704
θ range for data collection (deg)	1.3 to 25.0
Index ranges	-13<=h<=13, -18<=k<=18, -19<=l<=19
Reflections collected	23475
Independent reflections	9334 [R(int) = 0.0383]
Completeness to theta	99.9 %
Data/restraints/parameters	9334 / 21 / 775
F(000)	1218
Goodness-of-fit on F^2	1.039
Final *R* indices [I>2sigma(I)]	$R_1 = 0.0580$, w$R_2 = 0.1461$
R indices (all data)	$R_1 = 0.0855$, w$R_2 = 0.1719$
$\Delta\rho$ max,min (e·Å^{-3})	2.432 and -0.775

Table 3. Selected bond lengths [Å] and angles [°] for **3**.

N(1)-C(1)	1.365(6)	N(1)-C(4)-C(5)	125.7(5)
N(1)-C(4)	1.365(7)	N(1)-C(4)-C(3)	109.6(5)
N(2)-C(6)	1.362(7)	C(5)-C(4)-C(3)	124.6(5)
N(2)-C(9)	1.363(7)	C(4)-C(5)-C(6)	126.8(5)
N(3)-C(14)	1.364(6)	C(4)-C(5)-C(21)	117.4(5)
N(3)-C(11)	1.370(6)	C(6)-C(5)-C(21)	115.6(5)
N(4)-C(16)	1.364(7)	N(2)-C(6)-C(5)	125.5(5)
N(4)-C(19)	1.372(6)	N(2)-C(6)-C(7)	107.5(5)
C(1)-C(20)	1.401(7)	C(5)-C(6)-C(7)	126.9(5)
C(1)-C(2)	1.443(8)	C(8)-C(7)-C(6)	108.0(5)
C(2)-C(3)	1.330(8)	C(7)-C(8)-C(9)	107.8(5)
C(3)-C(4)	1.445(8)	N(2)-C(9)-C(10)	126.6(4)
C(4)-C(5)	1.383(8)	N(2)-C(9)-C(8)	107.2(5)
C(5)-C(6)	1.396(8)	C(10)-C(9)-C(8)	126.2(5)
C(5)-C(21)	1.504(7)	C(9)-C(10)-C(11)	124.7(5)
C(6)-C(7)	1.421(8)	C(9)-C(10)-C(27)	117.5(4)
C(7)-C(8)	1.349(8)	C(11)-C(10)-C(27)	117.5(5)
C(8)-C(9)	1.428(7)	N(3)-C(11)-C(10)	126.0(5)
C(9)-C(10)	1.396(7)	N(3)-C(11)-C(12)	109.8(4)
C(10)-C(11)	1.398(7)	C(10)-C(11)-C(12)	124.1(5)
C(10)-C(27)	1.489(7)	C(13)-C(12)-C(11)	107.3(5)
C(11)-C(12)	1.442(8)	C(12)-C(13)-C(14)	106.7(5)
C(12)-C(13)	1.340(8)	N(3)-C(14)-C(15)	125.2(5)
C(13)-C(14)	1.446(7)	N(3)-C(14)-C(13)	110.1(4)
C(14)-C(15)	1.398(7)	C(15)-C(14)-C(13)	124.6(5)
C(15)-C(16)	1.392(7)	C(16)-C(15)-C(14)	126.9(5)
C(15)-C(33)	1.499(7)	C(16)-C(15)-C(33)	116.5(4)
C(16)-C(17)	1.430(7)	C(14)-C(15)-C(33)	116.6(5)
C(17)-C(18)	1.347(8)	N(4)-C(16)-C(15)	125.3(5)
C(18)-C(19)	1.433(7)	N(4)-C(16)-C(17)	108.0(4)
C(19)-C(20)	1.391(7)	C(15)-C(16)-C(17)	126.7(5)
C(20)-C(39)	1.497(7)	C(18)-C(17)-C(16)	107.6(5)
C(32)-O(1)	1.377(7)	C(17)-C(18)-C(19)	108.2(5)
N(1S)-C(3B)	1.505(8)	N(4)-C(19)-C(20)	125.8(4)
N(1S)-C(4B)	1.507(8)	N(4)-C(19)-C(18)	107.3(4)
N(1S)-C(8B)	1.508(7)	C(20)-C(19)-C(18)	126.9(5)
N(1S)-C(6B)	1.522(7)	C(19)-C(20)-C(1)	126.1(5)
O(1)-C(1B)	1.425(9)	C(19)-C(20)-C(39)	116.8(4)
C(1B)-C(2B)	1.521(9)	C(1)-C(20)-C(39)	117.1(5)
C(2B)-C(3B)	1.522(9)	O(1)-C(32)-C(31)	119.7(5)
C(4B)-C(5B)	1.521(9)	O(1)-C(32)-C(27)	119.6(5)
C(6B)-C(7B)	1.505(10)	C(3B)-N(1S)-C(4B)	111.5(5)
C(8B)-C(9B)	1.525(9)	C(3B)-N(1S)-C(8B)	106.3(4)
		C(4B)-N(1S)-C(8B)	111.6(5)
		C(3B)-N(1S)-C(6B)	110.3(5)
C(1)-N(1)-C(4)	105.8(4)	C(4B)-N(1S)-C(6B)	106.3(4)
C(6)-N(2)-C(9)	109.4(4)	C(8B)-N(1S)-C(6B)	110.8(5)
C(14)-N(3)-C(11)	106.0(4)	C(32)-O(1)-C(1B)	116.0(5)
C(16)-N(4)-C(19)	108.9(4)	O(1)-C(1B)-C(2B)	106.9(6)
N(1)-C(1)-C(20)	125.2(5)	C(1B)-C(2B)-C(3B)	109.0(5)
N(1)-C(1)-C(2)	110.5(4)	N(1S)-C(3B)-C(2B)	115.3(5)
C(20)-C(1)-C(2)	124.3(5)	N(1S)-C(4B)-C(5B)	114.5(5)
C(3)-C(2)-C(1)	106.5(5)	C(7B)-C(6B)-N(1S)	114.2(5)
C(2)-C(3)-C(4)	107.6(5)	N(1S)-C(8B)-C(9B)	115.3(5)

Table 4. Hydrogen-bond geometry for **3** (Å, °)

Donor- H···Acceptor	D - H	H···A	D···A	D - H···A
N2-H2N···N1	0.70(9)	2.48(9)	2.913(7)	123(9)
N2-H2N···N3	0.70(9)	2.43(9)	2.897(7)	126(8)
N4-H4N···N1	0.75(9)	2.49(9)	2.895(7)	116(8)
N4-H4N···N3	0.75(9)	2.36(8)	2.905(6)	131(8)

8. Conformational analysis.

The porphyrin **3** adopts a "close" conformation in which the amino-alkyl side arm is folded toward the core of the macrocycle, with the terminal methyl groups of the pendant triethylammonium moiety pointing toward the pyrrole rings (I, II, IV). The lateral displacement of the side arm from the porphyrin centroid is generated by a gauche/anti/anti/anti(N)/anti conformation sequence along the main chain.

The porphyrin core is quasi-planar with an average deviation of the macrocycle atoms from their least squares plane ($\Delta24$, Table 5) of only 0.065 Å. The larger deviations are associated with the *meso*-carbon (C_m) C10 (0.106(5) Å) bonded to the para substituted aryl group and with the C_β of the neighbouring pyrrole rings (-0.089(6)-0.172(6) Å). Likewise, the C_α-C_m-C_α angle between the α-pyrrolic and *meso* carbons varies only slightly (Table 5) with the smallest value and the bigger deviation at *meso*-C10 position again (124.7(5)°).

The overall slightly distortion results essentially in a *saddle* shaped conformation characterized by an alternating displacement of the pyrrole rings N(I), (III) and (IV) below and above the mean plane (Figure 24).[9] A closer look of the out-of-plane distortion pattern suggests a small contribute from *wave* conformation involving the pyrrolic unit N(II) (toward which the side arm of porphyrin is bent).[10] The minor deformation from planarity of porphyrin macrocycle and the different role of the pyrrolic units is also reflected by the values of the dihedral angle between the pyrrole rings and the N_4-core mean plane (Table 5).

All the conformational data seem indicate that the small distortions observed for the macrocycle are essentially due to the presence and orientation of the "long" alkyl chain on the para position of a *meso*-aryl group. Despite the asymmetric substituent arrangement, the inner cavity shape composed by the four N atoms is square-like as indicated by the core elongation factor ($\Xi = 0.013$ Å) and by the distances between the neighbouring N-N atoms (2.895(7) – 2.913(7) Å). The N-H groups are involved in bifurcated N-H···(N,N) intramolecular hydrogen bonds (Table 4) and result only slightly tilted out of the plane of macrocycle.

Table 5. Selected conformational parameters for **3** (deviations and distances in Å, angles in °)

Core size $\otimes^a$	2.053	C_α-C_{15}-C_α	126.9(5)
Core elongation $\varXi^b$	0.013	C_α-C_{20}-C_α	126.1(5)
$\Delta24^c$	0.065	*cis* C_α-N$\cdots$N-$C_\alpha{}^g$	4.2
N1$\cdots$N2	2.913(7)	*trans* C_α-N$\cdots$N-C_α	177.1
N2$\cdots$N3	2.897(7)	φ_{pyr} N1^h	1.89
N3$\cdots$N4	2.905(6)	φ_{pyr} N2	7.24
N4$\cdots$N1	2.895(7)	φ_{pyr} N3	3.18
$\delta C_m{}^d$	0.074	φ_{pyr} N4	0.93
$\delta C_\alpha{}^e$	0.051	φ_{ar} C5^i	87.05
$\delta C_\beta{}^f$	0.102	φ_{ar} C10	87.87
C_α-C_5-C_α	126.8(5)	φ_{ar} C15	82.98
C_α-C_{10}-C_α	124.7(5)	φ_{ar} C20	81.15

C_m (*meso* carbon) = 5, 10, 15, 20; C_β (*β-pyrrole* position) = 2, 3, 7, 8, 12, 13, 17, 18; C_α (*α-pyrrole* position) = 1, 4, 6, 9, 11, 14, 16, 19. ^{a}The core size is defined as the geometrical centre of the four nitrogen atoms. ^{b}The core elongation parameter is defined as the difference between the vector lengths (|N1-N2|+|N3-N4|)/2 - (|N2-N3|+|N1-N4|)/2. ^{c}Deviation of the 24 macrocycle atoms from their least squares plane. ^{d}Average deviation of the C_m carbon atoms from the 4N plane. ^{e}Average deviation of the C_α atoms from the 4N plane. ^{f}Average deviation of the C_β atoms from the 4N plane. ^{g}Cis C_α –N–N– C_α dihedral angles.[11] ^{h}Pyrrole tilt angle with the 4N plane. ^{i}Phenyl tilt angle against the 4N plane.

Figure 24. Linear display of the skeletal deviations (in units of 0.001 Å) of the macrocycle atoms from the mean porphyrin plane (of 24 atom).[10] The *x* axis is not to scale.
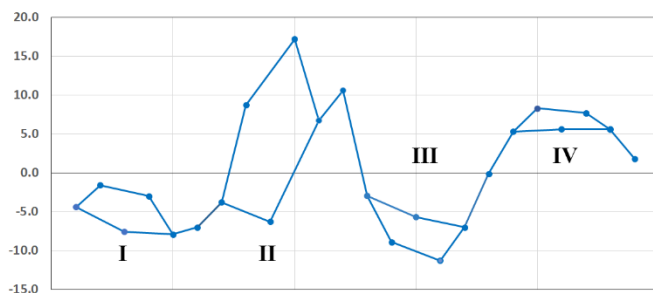
References

[1] T. A. D. Pinto, R. Hrdina, G. Kirsch, A. M. F. Oliveira-Campos, L. M. Rodrigues and A. P. Esteves, ARKIVOC 2012, **6**, 185-193

[2] H. G. Brittain, *Cryst. Growth Des.*, 2010, **10**, 1990-2003

[3] Bruker, *SAINT+*, 2007, Bruker AXS Inc., Madison, Wisconsin, USA.

[4] Bruker, APEX II, 2009, Bruker AXS Inc., Madison, Wisconsin, USA.

[5] M. C. Burla, R. Caliandro, M. Camalli, B. Carrozzini, G. L. Cascarano, L. De Caro, C. Giacovazzo, G. Polidori and R. Spagna, *J. Appl. Crystallogr.*, 2005, **38**, 381-388.

[6] G. M. Sheldrick, *Acta Crystallogr. Sect. C Struct. Chem.*, 2015, **71**, 3-8.

[7] L. J. Farrugia, *J. Appl. Crystallogr.*, 2012, **45**, 849-854.

[8] K. A. Connors: *Binding constants — the measurement of molecular complex stability*, John Wiley & Sons, New York 1987, 91, 1398-1398.

[9] M. Gruden, S. Grubišić, A. G. Coutsolelos and S. R. Niketić, *J. Mol. Struct.*, 2001, **595**, 209–224.

[10] a) W. Jentzen, X.-Z. Song and J. A. Shelnutt, *J. Phys. Chem. B*, 1997, **101**, 1684-1699; b) W. Jentzen, J.-G. Ma and J. A. Shelnutt, *Biophys. J.*, 1998, **74**, 753-763.

[11] A. Fidalgo-Marijuan, G. Barandika, B. Bazán, M.-K. Urtiaga and M. I. Arriortua, *CrystEngComm*, 2013, **15**, 4181.